Heliyon 6 (2020) e05338

Contents lists available at ScienceDirect

Heliyon

journal homepage: www.cell.com/heliyon

Research article

Viscous dissipation and joule heating effect on MHD flow and heat transfer past a stretching sheet embedded in a porous medium

B.K. Swain [a,*], B.C. Parida [b], S. Kar [c], N. Senapati [c]

[a] Department of Mathematics, IGIT, Sarang, Dhenkanal, Odisha 759146, India
[b] Department of Mathematics, Utkal University, BBSR, Odish 751004, India
[c] Department of Mathematics, Ravenshaw University, Cuttack, Odisha 753003, India

ARTICLE INFO

Keywords:
Mechanical engineering
MHD
HPM
Heat transfer
Viscous dissipation
Joule heating
Porous medium

ABSTRACT

An analysis is made to illustrate the MagnetoHydroDynamics (MHD) flow and gradient heat transport of a Newtonian fluid over a stretching sheet embedded in a porous matrix. The governing nonlinear partial differential equations are reconstituted as ordinary differential equations utilizing suitable similarity transformation and then treated numerically using 4^{th} order Runge-Kutta method along with shooting technique and analytically by Homotopy Perturbation Method. The verification of present study with earlier works serves as the benchmark of reliability of the present study. The important outcomes of this study are: porous parameter (K_p) acts as aiding force i.e when K_p is increased from 0.1 to 10 gradually there is a significant growth in velocity and after that rate of increment gets slowdown, greater Eckert number and joule heating parameter cause a rise in temperature as well as enhance the thermal boundary thickness. Consequently rate of heat transfer diminishes as thickness leads to low heat transfer coefficient. The applications of this study are shown in: multiple heating devices and industrial processes such as incandescent light bulb's filament emitting light, food processing and polymer processing etc.

1. Introduction

Acting as an energy source, viscous dissipation alters the temperature distributions which results to affect rate of heat transfer. The worthiness of the consequence of viscous dissipation confides in whether the plate is freezed or warmed. The joule heating also roles as a source of heat like the viscous dissipation in viscous fluid flow. Precisely, the deportment of heat towards synthesis of materials by ejection, paper manufacturing, cooling of electronic chips etc. are few real life applications where the ultimate product of required attributes builds upon cooling rate as well as stretching process.

Many authors have accomplished their research on the above discussed topic. Chaim [1] and Abel et al. [2] considered viscous and joules dissipation to study an electrically conducting fluid over a sheet that is linearly stretched. Analyzing the ohmic heating and viscous dissipation in his research, Chen [3] gave some fine results. Abo-Eldahab and Aziz [4] checked that how viscous dissipation and joules heating treat fluid flow for the case of power-law variation in wall temperature. A research on heat transfer flow of a second grade fluid has been looked over numerically by Bhargava and Singh [5] taking viscous dissipation and joule heating into consideration. Singh and Gorla [6] have illuminated the results of viscous dissipation and joule heating accomplishing a boundary layer analysis. Bandar Bin-Mohsin [7] has explored that how buoyancy respond when it is tested in MHD transport of Nanofluid. Venkateswarlu et.al [8] investigated Magnetohydrodynamics flow over a moving surface with constant heat source observing melting and viscous dissipation effects. The interpretation of Muhammad et.al [9] and Barlettaet.al [10] on the viscous dissipation also provide a better idea to the present researchers.

The joulean dissipation which is generated due to externally applied magnetic field interacting with conducting liquid, has significant application in many industries. Devi and Ganga [11] have evaluated a solution for MHD flow problem to check the impacts of viscous and joules dissipation. Barik et al. [12] have observed that how viscous dissipation affects MHD flow subject to power law heat flux. Khadijah [13] figured out the MHD flow and also inspected gradient heat transport phenomena. Viscous dissipation effect on Newtonian fluid flows have also been discussed by many researchers. Murugesan et al. [14] reported the outcomes of dissipative MHD nanofluid flow that is thermo-solutal stratified. The behaviour of MHD dissipative flow of Jeffrey Nanofluid has been

* Corresponding author.
E-mail address: bharatkeshari1@gmail.com (B.K. Swain).

https://doi.org/10.1016/j.heliyon.2020.e05338
Received 26 August 2020; Received in revised form 7 October 2020; Accepted 21 October 2020

elucidated by Sharma et.al [15]. Zueco [16] utilized network simulation method (NSM) to solve an unsteady MHD free convection flow problem and collected the information about the repercussion of viscous dissipation. Suneetha et al. [17, 18] have given some nice reports on the hydromagnetic flows by taking care of viscous dissipation. Recently some Authors ([Waini et al. [19], Mallick et al. [20], Seth et al [21], Megahed [22]) published their research works considering MHD flow past stretching sheet with joule heating and viscous dissipation, in very reputed journal.

Again, the impact of magnetic field on abovesaid flows in a porous medium are often seen in oil industries, extractions of energy, aerodynamics field etc. Thus, these kinds of engineering issues have been the area of interest for large number of eminent authors. Yadav and his co-authors [23, 24, 25, 26, 27] have nicely explained the impact of magnetic field on convective flow of Nanofluid in various types of porous layer. Sekhar et al. [28] illustrated the multiple slip effects considering the fluid flow in a porous medium. Makinde et al. [29, 30, 31] illuminated numerically the issues of MHD flows over many kinds of surfaces like vertical plate and stretching surface. They did their researches taking care of porous medium. Swain and Senapati [32] have expounded the impact of mass transfer on a free convective flow through a porous medium. Uddin [33] has also explicated the fluid flow over a stretching porous surface in a Porous Medium.

The intention of recent research is to figure out the results of viscous as well as joule dissipation on MHD flow and gradient heat transport past a stretching sheet set in a porous medium. The reduced ordinary differential equations are treated with HPM and 4th order RK-method with shooting technique. The aim of present investigation is to discuss the impacts of viscous and joulean dissipation which were not attended by Abualnajaby [13. However, Darcy dissipation which stems from the resistance offered by viscosity of the fluid and porous matrix of the saturated porous medium, has been neglected. Moreover, the works of Abualnajaby [13], Devi and Ganga [11] have been discussed as special cases. A good agreement of our result with earlier works serves as a bench mark of reliability. The present calculations and related graphs have been accomplished utilizing MATLAB.

2. Mathematical formulation

Consider a flow of an incompressible Newtonian fluid over an exponentially stretching sheet. The origin is located at the slit through which the sheet is drawn in the fluid medium as regarded by Mukhopadhyay [34]. The x-axis is delineated in the direction of sheet and y-axis is taken perpendicular to it. The surface is presumed to be stretched with the velocity $U = U_0 e^{x/L}$, where U_0 and L are the reference velocity and length respectively. The flow geometry is described in Figure 1.

A variable velocity v_w is included. The surface of the sheet is kept at a constant heat flux q_w and ambient fluid temperature T_∞. An external magnetic field $\overrightarrow{B_0}$ is applied parallel to y-axis. The external electrical field and the induced magnetic field are supposed to be negligible. Further, pressure gradient and hall current are assumed to be neglected. Subject to the above discussed presumptions and adopting the Boussinesq approximations, the governing boundary layer equations can be composed as

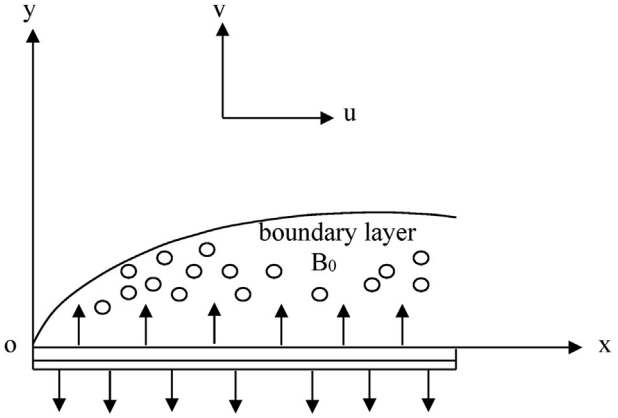

Figure 1. Flow geometry and coordinate system.

$$\frac{\partial u}{\partial x}+\frac{\partial v}{\partial y}=0, \tag{1}$$

$$u\frac{\partial u}{\partial x}+v\frac{\partial u}{\partial y}=\frac{\mu}{\rho}\frac{\partial^2 u}{\partial y^2}-\frac{\sigma B_0^2 u}{\rho}-\frac{\nu u}{K_p^*}, \tag{2}$$

$$u\frac{\partial T}{\partial x}+v\frac{\partial T}{\partial y}=\frac{k}{\rho C_p}\frac{\partial^2 T}{\partial y^2}-\frac{1}{\rho C_p}\frac{\partial q_r}{\partial y}+\frac{q'''}{\rho C_p}+\frac{\mu}{\rho C_p}\left(\frac{\partial u}{\partial y}\right)^2+\frac{\sigma B_0^2}{\rho C_p}u^2. \tag{3}$$

The boundary conditions are given by

$$u=U, v=-v_w, -k\left(\frac{\partial T}{\partial y}\right)=q_w \text{ at } y=0, \tag{4}$$

$$u\to 0, T\to T_\infty \text{ as } y\to\infty. \tag{5}$$

Here, it is assumed that $v_w = v_0 e^{x/2L}$, where v_0 is a constant.

According to Rosseland approximation ([35]), the radiative heat flux q_r is described as

$$q_r=-(4\sigma^*/3k^*)\frac{\partial T^4}{\partial y}. \tag{6}$$

Now as reported in [36], assuming the meager of the diversity in temperature in stream, expanding T^4 in a Taylor series about T_∞ and neglecting higher-order terms, we get

$$T^4\cong 4T_\infty^3 T-3T_\infty^4. \tag{7}$$

Introducing dimensionless coordinates

$$\eta=y\sqrt{\frac{U}{2\nu L}}, u=Uf'(\eta),\ v=-\sqrt{\frac{\nu U}{2L}}(f(\eta)+\eta f'(\eta)),\ \theta(\eta)=\frac{k}{q_w}(T-T_\infty)\sqrt{\frac{\mathrm{Re}}{2L^2}}$$

$$M=\frac{2\sigma B_0^2 L}{\rho U},\ P_r=\frac{\mu C_p}{k},\ R=\frac{16\sigma^* T_\infty^3}{3k^* k},\ f_w=v_0\left(\frac{\mu U_0}{2\rho L}\right)^{\frac{-1}{2}},\ K_p=\frac{K_p^* U}{2L\nu},\ \mathrm{Re}=\frac{UL}{\nu} \tag{8}$$

$$E_c=\frac{U^2 k}{C_p q_w}\sqrt{\frac{\mathrm{Re}}{2L^2}}, J=E_c M$$

and writting the internal heat generation or absorption q''' as (Chamkha and Khaled [37])

$$q'''=k\left(\frac{\mathrm{Re}}{2L^2}\right)[\mathrm{a}^*(T_w-T_\infty)e^{-\eta}+b^*(T-T_\infty)], \tag{9}$$

the governing Eqs. (1), (2), and (3) with the help of Eqs. (6) and (7) can be reduced to the following non-dimensional form:

$$f'''+ff''-2f'^2-\left(M+\frac{1}{K_p}\right)f'=0, \tag{10}$$

$$(1+R)\theta''+P_r(\theta f'+\theta' f)+\mathrm{a}^* e^{-\eta}+b^*\theta+E_c P_r f''^2+JP_r f'^2=0. \tag{11}$$

The transformed boundary conditions are

$$f=f_w, f'=1,\ \theta'=-1,\ \text{at } \eta=0, \tag{12}$$

$$f'\to 0, \theta\to 0 \text{ as } \eta\to\infty. \tag{13}$$

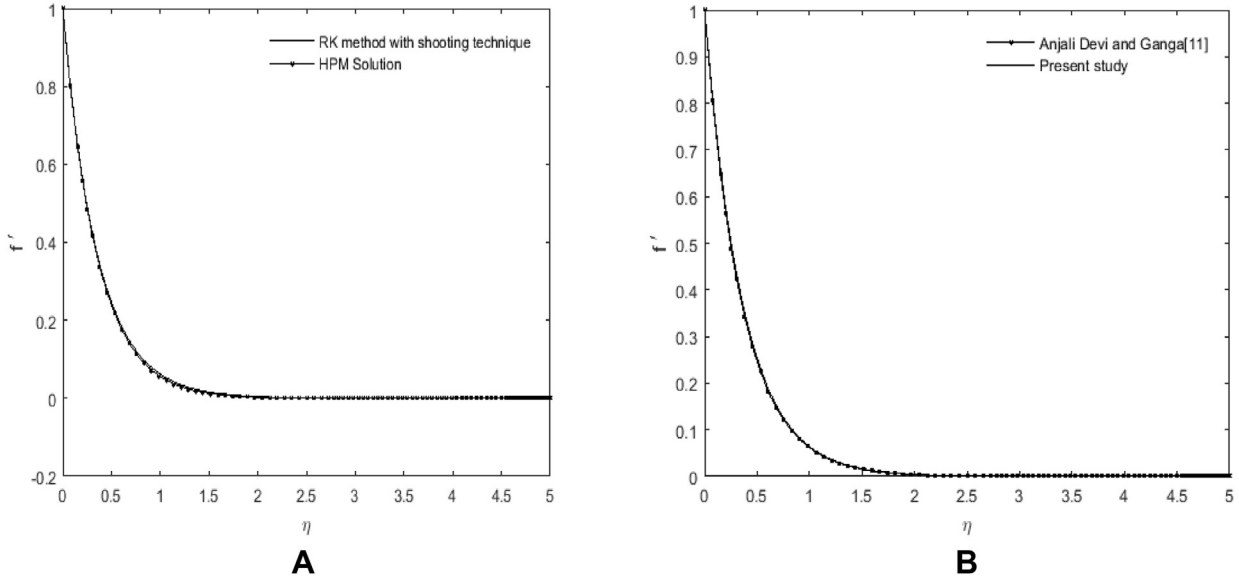

Figure 2. Comparison of present solution for velocity by RK method with HPM method and previous result [11].

Again there exist physical quantities which are called the skin friction coefficient which is proportional to $-f''(0)$ and the Nusselt number which is proportional to $\frac{1}{\theta(0)}$.

3. Method of solution

The Eqs. (10) and (11) are solved analytically as well as numerically under the boundary conditions (12) and (13).

(i) Solution by Homotpy perturbation method (HPM)

To interpret HPM, the non-linear differential equation is assumed as

$$A(u) - f(r) = 0, r \in \Omega \tag{14}$$

with the boundary conditions

$$B\left(u, \frac{\partial u}{\partial \eta}\right) = 0, r \in \Gamma, \tag{15}$$

where A, a differential operator, B, a boundary operator, f(r), a known analytical function and Γ, boundary of the domain Ω. A can be illustrated by linear and nonlinear parts. So Eq. (14) is rewritten as follows:

$$L(u) + N(u) - f(r) = 0, r \in \Omega. \tag{16}$$

By the HPM technique, a homotopy is estimated as

$$v(r, q) : \Omega \times [0, 1] \rightarrow R$$

which satisfies:

Table 1. Comparison with earlier results.

Taking R = 0.5, P_r = 1, M = 1, a* = 0.2, b^* = 0.2		
	Previous result by Khadijah [13] $f''(0)$	Present result $f''(0)$
M = 0	-2. 20348	-2.203913
M = 1.5	-2.65822	-2.658565
$f_w = 1$	-2.02809	-2.028286
$f_w = 2$	-2.74565	-2.745943

$$H(v, q) = (1 - q)[L(v) - L(u_0)] + q[A(v) - f(r)] = 0, q \in [0, 1], r \in \Omega \tag{17}$$

where $q \in [0, 1]$ is an embedding parameter and u_0 is an initial approximation satisfying the boundary. Thus

$$H(v, 0) = L(v) - L(u_0) = 0$$
$$H(v, 1) = A(v) - f(r) = 0$$

The change of q from zero to one is just that of $v(r, p)$ from $u_0(r)$ to $u(r)$. In HPM, a small embedding parameter is used and it is presumed that the solution is a power series in q. With this consideration we obtain

$$v = v_0 + qv_1 + q^2v_2 + \ldots\ldots \tag{18}$$

As $q \rightarrow 1$, (18) gives the approximate solution of (14) which is given by

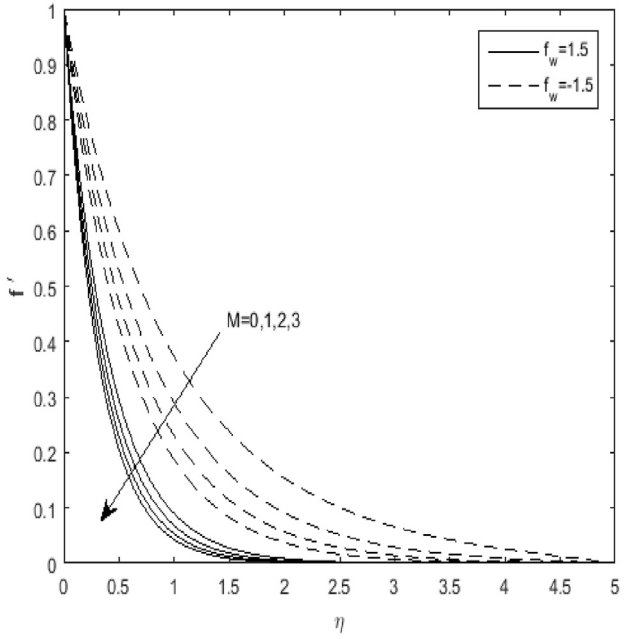

Figure 3. Velocity profiles for M when R = 0.5, $P_r = 1$, $K_p = 1$, $E_c = 0.02$, a* = 0.2, $b^* = 0.2$, $P_r = 1$.

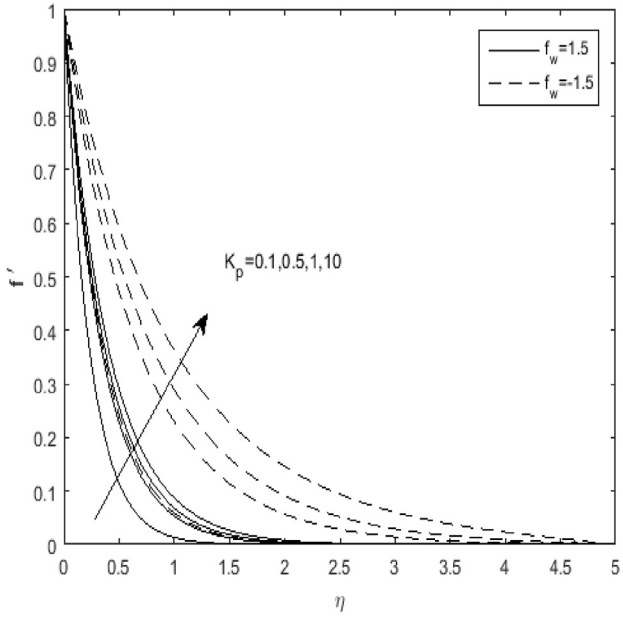

Figure 4. Velocity profiles for K_p when $P_r = 1$, R = 0.5, M = 1, $E_c = 0.02$, a* = 0.2, $b^* = 0.2$.

$$u = \lim_{q\to 1} v = v_0 + v_1 + v_2 + \ldots\ldots \tag{19}$$

This method is convergent and stable which is clearly illuminated by He [38].

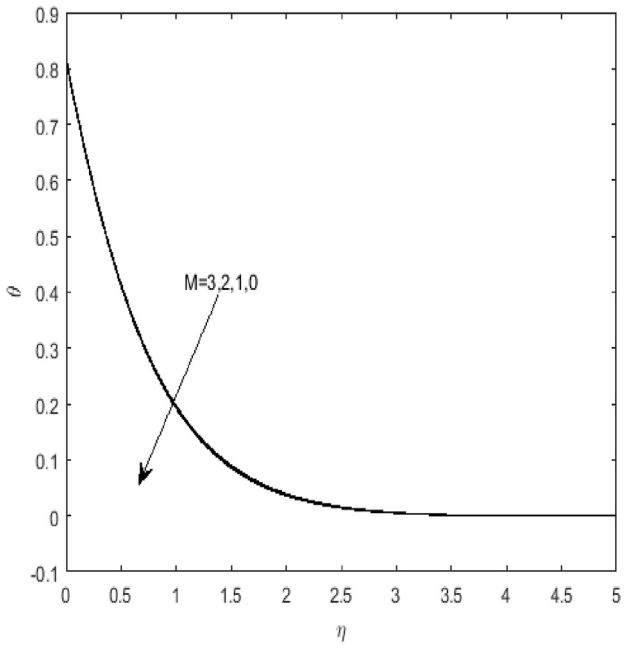

Figure 6. Temperature profiles for M when R = 0.5 $P_r = 1$, $E_c = 0.02$, $K_p = 1$, a* = 0.2, $b^* = 0.2$, $f_w = 1.5$.

$$(1-q)\left(f''' - \left(M + \frac{1}{K_p}\right)f'\right) + q\left(f''' + ff'' - 2f'^2 - \left(M + \frac{1}{K_p}\right)f'\right) = 0 \tag{20}$$

$$(1-q)((1+R)\theta'' + ae^{-\eta} + b\theta) + q\left((1+R)\theta'' + P_r\theta f' + P_r\theta' f + ae^{-\eta} + b\theta + E_c P_r f''^2 + JP_r f'^2\right) = 0 \tag{21}$$

Here we set (10) and (11) into the following form by introducing 'q' as homotopy perturbation parameter

Now putting $f = f_0 + qf_1 + q^2 f_2 + \cdots, \theta = \theta_0 + q\theta_1 + q^2\theta_2 + \cdots$ in (20) and (21)

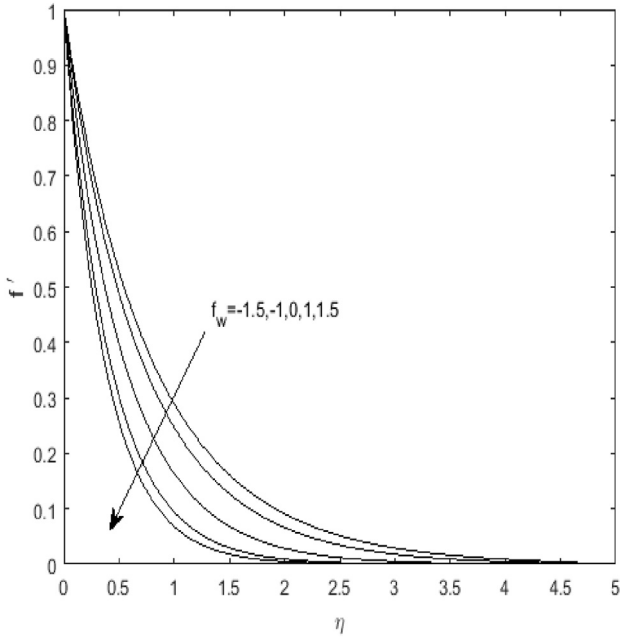

Figure 5. Velocity profiles for f_w when R = 0.5, $P_r = 1$, $E_c = 0.02$, a* = 0.2, $b^* = 0.2$, $K_p = 1$, M = 1.

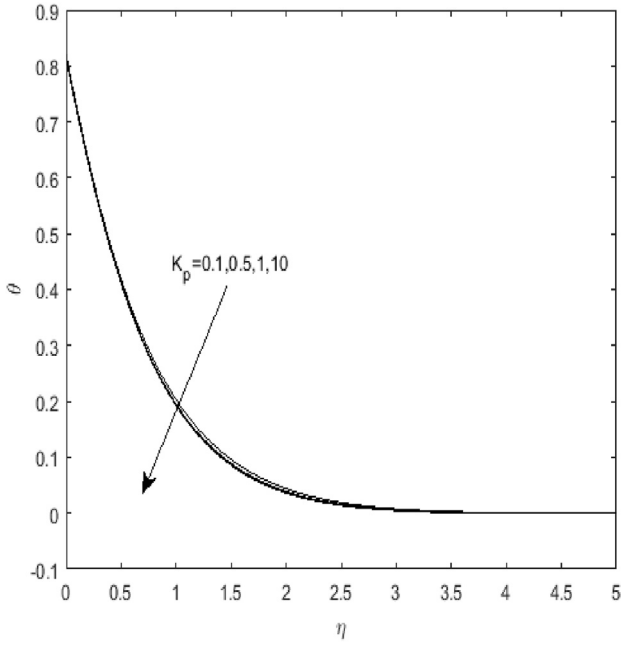

Figure 7. Temperature profiles for K_p when R = 0.5, $P_r = 1$, M = 1, $E_c = 0.02$, a* = b* = 0.2, $f_w = 1.5$.

and collecting the coefficients of q^0 and q^1, we get

$$f_0''' - \left(M + \frac{1}{K_p}\right) f_0' = 0, \tag{22}$$

$$f_1''' - \left(M + \frac{1}{K_p}\right) f_1' = -f_0 f_0'' + 2f_0'^2, \tag{23}$$

$$(1+R)\theta_0'' + ae^{-\eta} + b\theta_0 = 0, \tag{24}$$

$$(1+R)\theta_1'' + b\theta_1 = -P_r\theta_0 f_0' - P_r\theta_0' f_0 - E_c P_r f_0''^2 - JP_r f_0'^2. \tag{25}$$

The boundary conditions (12) and (13) are reduced to

$$f_0 = f_w, f_0' = 1, \theta_0' = -1, f_1 = 0, f_1' = 1, \theta_1' = 0 \text{ at } \eta = 0 \tag{26}$$

$$f_0' \to 0, f_1' \to 0, \theta_0 \to 0, f, \theta_1 \to 0 \; as \; \eta \to \infty \tag{27}$$

Solving Eqs. (22), (23), (24), and (25) under the boundary conditions (26) and (27), f_0 and f_1 are obtained. Here η_∞ is taken as 5.

The HPM iterative process is considered upto first order. Hence $f = \lim_{q\to 1}(f_0 + qf_1)$ and $\theta = \lim_{q\to 1}(\theta_0 + q\theta_1)$.

(ii) Runge-Kutta method with shooting technique

The coupled nonlinear Eqs. (10) and (11) subject to the boundary conditions (12) and (13) are solved using the fourth order Runge-Kutta method with shooting technique.

The coupled nonlinear Eqs. (10) and (11) with the boundary conditions (12) and (13) are treated using the fourth order Runge-Kutta method with shooting technique. The Eqs. (10) and (11) are converted to a set of first order differential equations substituting

$$f = y_1, f' = y_2, f'' = y_3, \theta = y_4, \theta' = y_5. \tag{28}$$

The reduced equations are

$$y_3' = -y_1 y_3 + 2y_2^2 + \left(M + \frac{1}{K_p}\right) y_2, \tag{29}$$

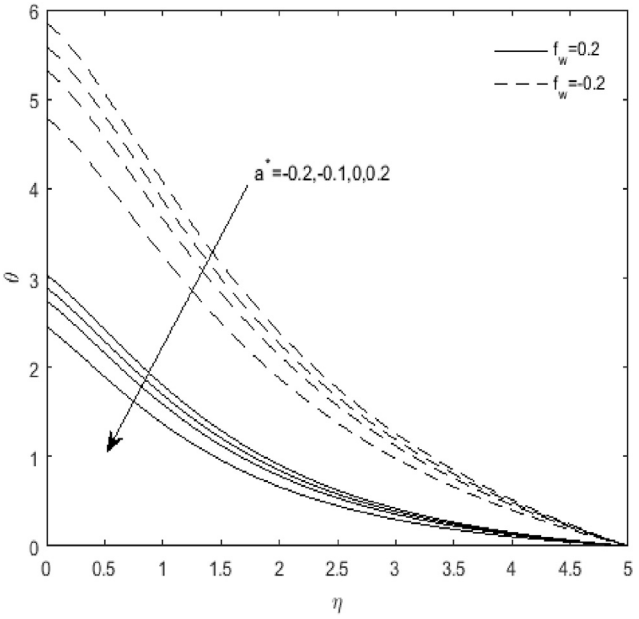

Figure 9. Temperature profiles for a* when R = 0.5, $P_r = 1$, M = 1, $E_c = 0.02$, $b^* = 0.2$, $K_p = 1$.

$$y_5' = \left(\frac{1}{1+R}\right)\left(-P_r(y_2 y_4 + y_5 y_1) - a^* e^{-\eta} - b^* y_4 - E_c P_r y_3^2 - J\text{Pr}y_2^2\right). \tag{30}$$

Respective boundary conditions are obtained as

$$y_1 = f_w, y_2 = 1, y_3 = ?, \; y_5 = -1, y_4 = ? \text{ at } \eta = 0, \tag{31}$$

$$y_2 \to 0, y_4 \to 0 \text{ as } \eta \to \infty. \tag{32}$$

For integrating, y_3 and y_4 at $\eta = 0$ are guessed and the step by step integration is accomplished with step length 0.01 using shooting technique with MATLAB code having error bound 10^{-3}.

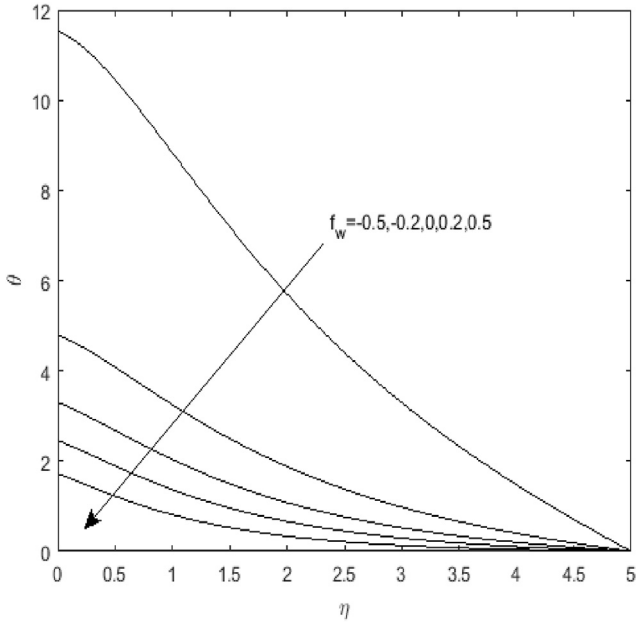

Figure 8. Temperature profiles for f_w, R = 0.5 $P_r = 1$, M = 1, $E_c = 0.02$, a* = b* = 0.2, $K_p = 1$.

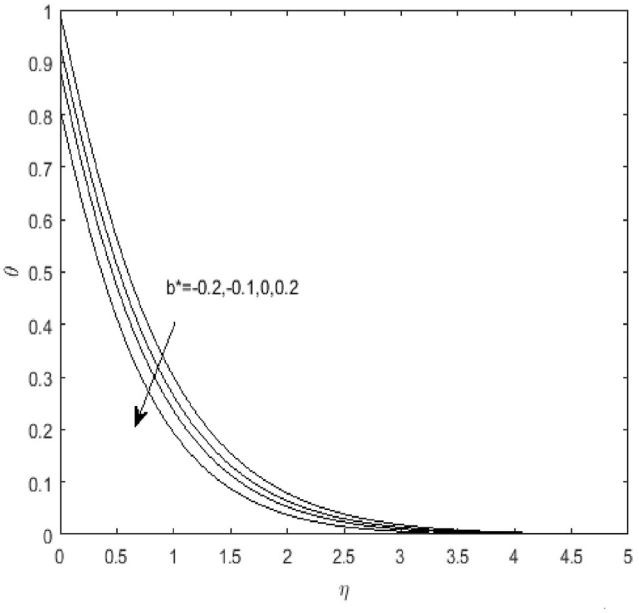

Figure 10. Temperature profiles for b* when R = 0.5, =1, M = 1, $E_c = 0.02$, f_w = 1.5, a* = 0.2, $K_p = 1$.

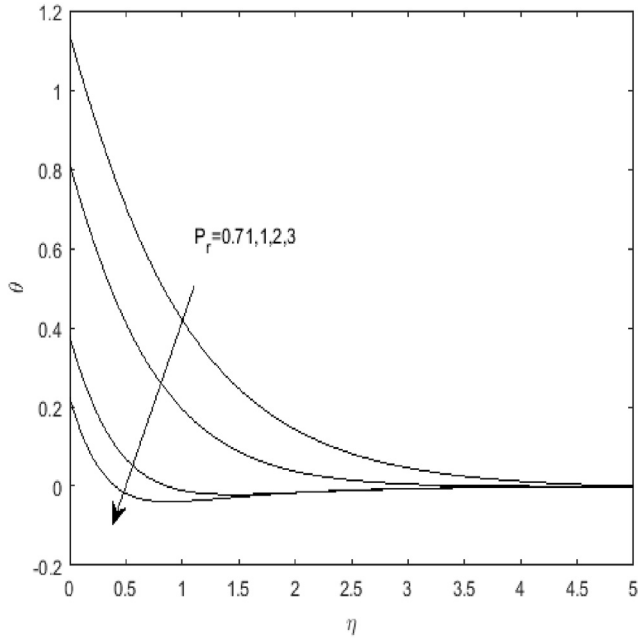

Figure 11. Temperature profiles for P_r when $P_r = 1$, M = 1, $E_c = 0.02$, R = 0.5, $b^* = 0.2$, $K_p = 1$,$f_w = 1.5$.

4. Validation

To validate our calculation, the numerical solution for velocity (for M = 1, $K_p = 0.2$, $f_w = 0.2$) obtained by 4th order Runge-Kutta method with shooting technique is compared with HPM solution in Figure 2(a) which shows a good agreement. Again Figure 2(b) compares the present numerical solution with the exact solution obtained by Devi and Ganga [11]. The exact solution for f is given by

$$f(\eta) = \frac{1}{\alpha}\left[\alpha^2 - \left(M + \frac{1}{K_p}\right) - e^{-\alpha\eta}\right] \quad \text{where } \alpha = \frac{f_w + \sqrt{\alpha^2 + 4\left(1 + M + \frac{1}{K_p}\right)}}{2}.$$

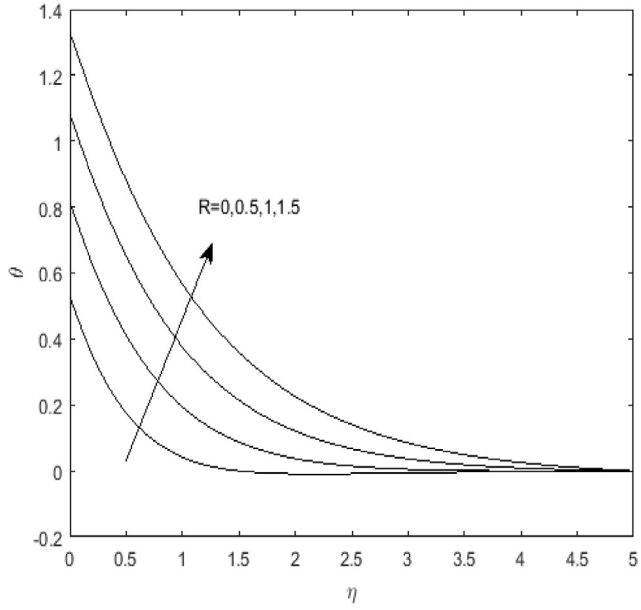

Figure 12. Temperature profiles for R when M = 1,$E_c = 0.02$, $f_w = 1.5$, a* = 0.2, $P_r = 1$, a* = 0.2, $b^* = 0.2$, $K_p = 1$.

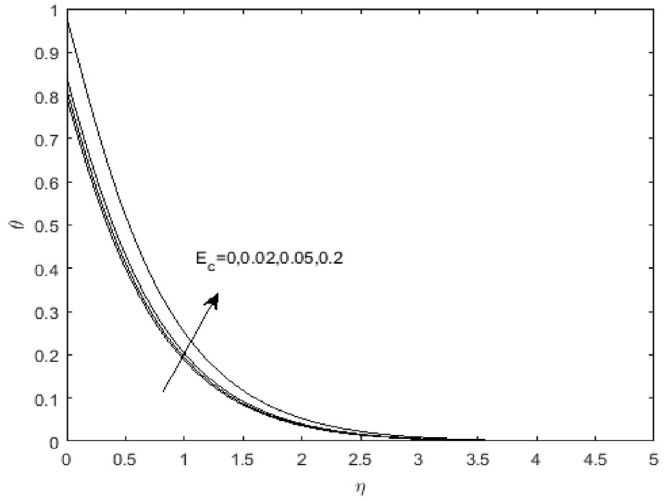

Figure 13. Temperature profiles for E_c when R = 0.5, $P_r = 1$, M = 1, $f_w = 1.5$, a* = 0.2, $b^* = 0.2$, $K_p = 1$.

Finally, our results (for$K \to \infty, E_c = 0$) are compared with the previous DTM solutions given by Khadijah [13] in Table 1. The comparisons discussed here prove the accuracy of our mode of calculation.

5. Results and discussion

The effects of different physical parameters such as magnetic parameter, suction parameter, Prandtl number, Nusselt number etc. are discussed elaborately. The values of the parameters used in the computation following [13], are as follows:

M = 1,R = 0.5, $K_p = 1$, $E_c = 0.02$, a* = 0.2, $b^* = 0.2$, $P_r = 1$, $f_{w=}1.5$.

Figure 3 represents the influence of Magnetic parameter, M on velocity profile. It is found that velocity diminishes when the magnetic parameter increases as in previous study [13]. A kind of drag-like force called Lorentz force is produced by the conducting fluid, which causes a reduction in the fluid velocity. In both the case (suction (f_w>0) and injection (f_w<0)), same trend is found. Due to resistive force generated and acted upon the main directional flow, the velocity decreases. Again for low intensity magnetic field, the significant increase in velocity is marked. Therefore, during clinical or mechanical necessity to control the flow of fluid, one can regulate the intensity of the external magnetic field to obtain the desired flow rate.

In Figure 4, K_p acts as aiding force for the fluid velocity i.e. the increasing values of K_p enhances the velocity for suction as well as for injection. On careful observation, again it is found that when K_p is increased from 0.1 to 10, gradually there is a significant growth in velocity and after that rate of increment gets slowdown.

Figure 5 reveals when the suction parameter f_w increases, velocity diminishes. So we can also control the flow through suction. The same

Table 2. Skin data.

Sl. No.	M	K_p	f_w	$f''(0)$
1	0	1	1.5	-2.52073
2	0.5	1	1.5	-2.65853
3	1	1	1.5	-2.78669
4	1.5	1	1.5	-2.90702
5	1	1	1	-2.46362
6	1	1	2	-3.13759
7	1	0.1	1.5	-4.38096
8	1	0.5	1.5	-3.02082
9	1	10	1.5	-2.54918

Table 3. Nusselt number data.

Sl.No.	M	K_p	f_w	P_r	E_c	R	a^*	b^*	$1/\theta(0)$
1	0	1	1.5	1	0.02	0.5	0.2	0.2	1.23311
2	1	1	1.5	1	0.02	0.5	0.2	0.2	1.22811
3	1.5	1	1.5	1	0.02	0.5	0.2	0.2	1.22590
4	1	0.1	1.5	1	0.02	0.5	0.2	0.2	1.21810
5	1	0.5	1.5	1	0.02	0.5	0.2	0.2	1.22681
6	1	1	1	1	0.02	0.5	0.2	0.2	0.89201
7	1	1	2	1	0.02	0.5	0.2	0.2	1.57559
8	1	1	1.5	0.71	0.02	0.5	0.2	0.2	0.87759
9	1	1	1.5	2	0.02	0.5	0.2	0.2	2.63769
10	1	1	1.5	1	0	0.5	0.2	0.2	1.25641
11	1	1	1.5	1	0.03	0.5	0.2	0.2	1.21444
12	1	1	1.5	1	0.02	1	0.2	0.2	0.92431
13	1	1	1.5	1	0.02	1.5	0.2	0.2	0.75217
14	1	1	1.5	1	0.02	0.5	-0.1	0.2	1.02445
15	1	1	1.5	1	0.02	0.5	0	0.2	1.08439
16	1	1	1.5	1	0.02	0.5	0.3	0.2	1.31527
17	1	1	1.5	1	0.02	0.5	0.2	-0.1	1.06830
18	1	1	1.5	1	0.02	0.5	0.2	0	1.12590
19	1	1	1.5	1	0.02	0.5	0.2	0.3	1.27427

behaviour is shown in the study of Khadijah [13]. This gives the accuracy of present study.

From Figures 6 and 7, the effects of magnetic parameter, M and porosity parameter K_p on temperature profile are found. It is noted that magnetic parameter is directly proportional to the temperature whereas K_p adversely affect the temperature. Increasing values of K_p yields lower temperature. Again for magnetic parameter, the curves are very close to each other which represent the effect of M on temperature is not so significant.

In Figures 8, 9 and 10, f_w, a* and b^* have the same influence on temperature distribution. Temperature sharply reduces as these parameters are increased. $a^* < 0, b^* < 0$ helps to raise the temperature and $a^* > 0, b^* > 0$causes a fall in temperature. This result is just opposite to that of Khadijah [13]. Again it is clear that less the injection more the temperature and more the suction less the temperature. Again temperature approaches to zero slowly in case of injection compared to that in case of suction.

Figure 11 gives the effect of Prandtl numer P_r on temperature. Various values of P_r are taken for industrial/engineering importance, namely $P_r = 0.71$, $P_r = 1$, $P_r = 2$, $P_r = 3$ which correspond to air, electrolyte solutions, water at 60^0c respectively. It is noted that increase in Prandtl number results a fall in the temperature. Prandtl number represents the ratio of momentum and thermal diffusivities. Lower P_r valued fluid corresponds to gases of low density and higher P_r valued fluids are connected with denser fluids. Hence an increase in P_r serves to strongly reduction in temperature. This finding is in agreement with Khadijah [13].

In Figure 12, temperature is significantly increased with increase in radiation parameter R. So the radiation parameter thickens the thermal boundary and also enables the fluid to release heat energy from the flow region to make the system cool. Figure 13 describes the outcome of Eckert number (E_c). As Eckert number comes from kinetic energy of flow and heat enthalpy difference, so improve in Eckert number enhances kinetic energy. Again it is known that temperature is considered as average kinetic energy. Greater viscous dissipative heat rises the temperature. Thus we can say that temperature of the fluid rises. From this graph, it is analyzed that fluid temperature rises as E_c is increased.

Furthermore, Joule heating parameter is taken as $J = E_c M$, so increase in E_c and M results an increase in joule heating parameter. Since larger values of Eckert number and magnetic parameter help to raise the temperature, thus it can be illuminated that higher values of Joule heating parameter aid to upsurge in temperature.

In Table 2, we analyzed that how the parameters f_w, M, K_p affect skin friction. It is clear that increasing values of porosity parameter enhance the skin friction whereas magnetic parameter and suction parameter are indirectly proportional to the skin friction.

Table 3 represents the various numerical values of Nusselt number to analyze the influences of different parameters. It is observed that increasing values of R, M and E_c reduce the Nusselt number and rest of the parameters are directly proportional to it.

6. Conclusion

The problem of an incompressible Newtonian fluid flow is solved using the fourth order Runge-Kutta method with shooting technique. The presence of viscous dissipation and joule heating is discussed elaborately. As a special case ($K_p \to \infty, E_c = 0$), our results are compared with the previous DTM solutions [13] and a very good agreement is found. Some nice results are also given below.

- Improve in the Eckert number (E_c) is to raise the temperature distribution. So it can be said that the energy is accumulated in the fluid region as a consequence of dissipation.
- The radiation parameter helps for thickening the thermal boundary layer.
- Positive values of heat generation/absorption parameters reduce the temperature whereas negative values enhance it.
- Higher Magnetic parameter and suction parameter diminish the fluid flow velocity. On the other hand, increasing values of Porosity parameter gives higher velocity.
- When thermal diffusivity dominates momentum diffusivity, temperature rises.
- Lager viscous dissipation and joule heating parameter reduce the heat transfer.

- Porous parameter K_p enhances Nusselt number.
- Magnetic parameter adversely affects the shearing stress.

Declarations

Author contribution statement

B. K. Swain & N. Senapati: Conceived and designed the experiments; Performed the experiments; Analyzed and interpreted the data; Contributed reagents, materials, analysis tools or data; Wrote the paper.

B. C. Parida: Conceived and designed the experiments; Performed the experiments; Analyzed and interpreted the data; Contributed reagents, materials, analysis tools or data.

S. Kar: Conceived and designed the experiments; Performed the experiments; Analyzed and interpreted the data; Wrote the paper.

Funding statement

This research did not receive any specific grant from funding agencies in the public, commercial, or not-for-profit sectors.

Competing interest statement

The authors declare no conflict of interest.

Additional information

No additional information is available for this paper.

References

[1] T.C. Chaim, Magnetohydrodynamic heat transfer over a non-isothermal stretching sheet, Acta Mech. 122 (1977) 169–179.
[2] M.S. Abel, E. Sanjayan, Nadeppanvar, Viscoelastic MHD flow and heat transfer over a stretching sheet with viscous and ohmic dissipations, Commun. Nonlinear Sci. Numer. Simulat. 13 (2008) 1808–1821.
[3] C.H. Chen, Combined heat and mass transfer in MHD free convection from a vertical surface with ohmic heating and viscous dissipation, Int. J. Eng. Sci. 42 (2004) 699–713.
[4] E.M. Abo-Eldahab, M.A. El Aziz, Viscous dissipation and joules heating effects on MHD free convection from a vertical flat plate with power-law variation in surface temperature in the presence of Hall and non-slip currents, Appl. Math. Model. 29 (2005) 579–595.
[5] R. Bhargava, S. Singh, Numerical simulation of unsteady MHD flow and heat transfer of a second grade fluid with viscous dissipation and Joule heating using meshfree approach, World Acad. Sci. Eng. Technol. 67 (2012) 1043–1049.
[6] A.K. Singh, R.S.R. Gorla, Free convective heat and mass transfer with Hall current, Joule heating and thermal diffusion, Heat Mass Tran. 45 (11) (2009) 1341–1349.
[7] B.M. Bandar, Buoyancy effects on MHD transport of Nanofluid over a stretching surface with variable viscosity, IEEE Access 7 (2019) 75398–75406.
[8] B. Venkateswarlu, P.V. Satya Narayana, N. Tarakaramu, Melting and viscous dissipation effects on MHD flow over a moving surface with constant heat source, Trans. A Razmadze Math. Inst. 172 (2018) 619–630.
[9] T. Muhammad, S. AliShehzad, A. Alsaedi, Viscous dissipation and Joule heating effects in MHD 3D flow with heat and mass fluxes, Results in Physics 8 (2018) 365–371.
[10] A. Barletta, M. Celli, Mixed convection MHD flow in a vertical channel with joules and viscous dissipation effects, Int. J. Heat Mass Tran. 5 (2008) 6110–6117.
[11] S.P. Anjali Devi, B. Ganga, Effects of viscous and joules dissipation on MHD flow, heat and mass transfer past a stretching porous surface embedded in a porous medium, Nonlinear Anal. Model Contr. 14 (2009) 303–314.
[12] R.N. Barik, G.C. Dash, P.K. Rath, MHD flow and heat transfer over a stretching porous sheet subject to power law heat flux in the presence of chemical reaction and viscous dissipation, Int. J. Comput. Sci. Math. 4 (2013) 252–265.
[13] M.A. Kadijah, Numerical studies for MHD flow and gradient heat transport past a stretching sheet with radiation and heat production via DTM, Appl. Appl. Math 13 (2018) 915–924.
[14] T. Murugesan, M. Dinesh Kumar, Viscous dissipation and Joule heating effects on MHD flow of a Thermo-Solutal stratified nanofluid over an exponentially stretching sheet with radiation and heat generation/absorptionInt, World Sci. J. 129 (2019) 193–210.
[15] K. Sharma, S. Gupta, Viscous dissipation and thermal radiation effects in MHD flow of Jeffrey nanofluid through impermeable surface with heat generation/absorption, Nonlinear Eng. 6 (2017) 153–166.
[16] J. Zueco Jordan, Network simulation method applied to radiation and dissipation effects on MHD unsteady free convection over vertical porous plate, Appl. Math. Model. 31 (2007) 2019–2033.
[17] S. Suneetha, N. Bhaskar Reddy, V. Ramachandra Prasad, The thermal radiation effects on MHD free convection flow past an impulsively started vertical plate with variable surface temperature and concentration, J. Nav. Architect. Mar. Eng. 2 (2008) 57–70.
[18] S. Suneetha, N. Bhaskar Reddy, V. Ramachandra Prasad, Radiation and mass transfer effects on MHD free convection flow past an impulsively started isothermal vertical plate with dissipation, Therm. Sci. 13 (2009) 71–181.
[19] I. Waini, A. Ishak, I. Pop, MHD flow and heat transfer of a hybrid nanofluid past a permeable stretching/shrinking wedge, Appl. Math. Mech. 41 (2020) 507–520.
[20] B. Mallick, J.C. Misra, A.R. Chowdhury, Influence of Hall current and Joule heating on entropy generation during electrokinetically induced thermoradiative transport of nanofluids in a porous microchannel, Appl. Math. Mech. **40** (2019) 1509–1530.
[21] G.S. Seth, R. Tripathi, M.K. Mishra, Hydromagnetic thin film flow of Casson fluid in non-Darcy porous medium with Joule dissipation and Navier's partial slip, Appl. Math. Mech. 38 (2017) 1613–1626.
[22] A.M. Megahed, Carreau fluid flow due to nonlinearly stretching sheet with thermal radiation, heat flux, and variable conductivity, Appl. Math. Mech. 40 (2019) 1615–1624.
[23] D. Yadav, The density-driven nanofluid convection in an anisotropic porous medium layer with rotation and variable gravity field: a numerical investigation, J. Appl. Comput. Mech. 6 (2020) 699–712.
[24] D. Yadav, J. Wang, Convective heat transport in a heat generating porous layer saturated by a non-Newtonian nanofluid, Heat Tran. Eng. 40 (2019) 1363–1382.
[25] D. Yadav, The effect of pulsating through flow on the onset of magneto convection in a layer of nanofluid confined within a Hele-Shaw cell, Proc. IME E J. Process Mech. Eng. 233 (2019) 1074–1085.
[26] D. Yadav, J. Wang, R. Bhargava, J. Lee, H.H. Cho, Numerical investigation of the effect of magnetic field on the onset of nanofluid convection, Appl. Therm. Eng. 103 (2016) 1441–1449.
[27] D. Yadav, Impact of chemical reaction on the convective heat transport in nanofluid occupying in porous enclosures: a realistic approach, Int. J. Mech. Sci. 157 (2019) 357–373.
[28] K.R. Sekhar, G.V. Reddy, C.S.K. Raju, S.M. Ibrahim, O.D. Makinde, Multiple slip effects on magnetohydrodynamic boundary layer flow over a stretching sheet embedded in a porous medium with radiation and Joule heating, Spec. Top Rev. Porous Media Int. J. 9 (2018) 117–132.
[29] O.D. Makinde, Z.H. Khan, R. Ahmad, W.A. Khan, Numerical study of unsteady hydromagnetic radiating fluid flow past a slippery stretching sheet embedded in a porous medium, Phys. Fluids 30 (2018), 083601-7.
[30] O.D. Makinde, W.A. Khan, Z.H. Khan, Analysis of MHD nanofluid flow over a convectively heated permeable vertical plate embedded in a porous medium, J. Nanofluids 5 (2016) 574–580.
[31] W.N. Mutuku-Njane, O.D. Makinde, Combined effect of buoyancy force and Navier Slip on MHD flow of a nanofluid over a convectively heated vertical porous plate, Sci. World J. (2013) 1–8. Article ID 725643.
[32] B.K. Swain, N. Senapati, The effect of mass transfer on mhd free convective radiating flow over an impulsively started vertical plate embedded in a porous medium, J. Appl. Anal. Comput. 5 (2015) 18–27.
[33] M.S. Uddin, Viscous and joules dissipation on MHD flow past a stretching porous surface embedded in a porous medium, J. Appl. Math. Phys. 3 (2015) 1710–1725.
[34] S. Mukhopadhyay, MHD boundary layer flow and heat transfer over an exponentially stretching sheet embedded in a thermally stratified medium, Alexandria Eng. J. 52 (2013) 259–265.
[35] A. Raptis, Flow of a micropolar fluid past a continuously moving plate by the presence of radiation, Int. J. Heat Mass Tran. 41 (1998) 2865–2866.
[36] A. Raptis, Radiation and viscoelastic flow, Int. Commun. Heat Mass Tran. 26 (1999) 889–895.
[37] A.J. Chamkha, A.A. Khaled, Similarity solutions for hydromagnetic simultaneous heat and mass transfer by natural convection from an inclined plate with internal heat generation or absorption, Heat Mass Tran. 37 (2001) 117–123.
[38] J.H. He, Homotopy perturbation method for bifurcation of nonlinear problems, Int. J. Nonlinear Sci. Numer. Stimul. 6 (2) (2005) 207–208.